Electronic Supporting Information

Lanthanide and Actinide doped $B_{12}H_{12}^{2-}$ and $Al_{12}H_{12}^{2-}$ Clusters: New Magnetic Superatoms with f-block Elements

Meenakshi Joshi[#,†] and Tapan K. Ghanty[#,†,*]

[#]*Theoretical Chemistry Section, Chemistry Group, Bhabha Atomic Research Centre, Mumbai 400085, India*

[†]*Homi Bhabha National Institute, Training School Complex, Anushakti Nagar, Mumbai–400094, India*

AUTHOR INFORMATION

Corresponding Author

[*]Email: tapang@barc.gov.in; Fax: 0091–22–25505151

List of Tables

<u>List of Figures</u>

Figure S5. Density of state (DOS) plots of (a) $Pu@Al_{12}H_{12}$ and (b) $Sm@Al_{12}H_{12}$, septet spin exohedral clusters at B3LYP/DEF, PBE/DEF, M06-2X/DEF and TPSSH/DEF level of theory

Figure S6. Density of state (DOS) of spin up (alpha) and spin down (beta) plots of (a) $An@Al_{12}H_{12}^{2-}$ (An = Pu^{2+}, Am^{3+}) and (b) $Ln@Al_{12}H_{12}^{2-}$ (Ln = Sm^{2+}, Eu^{3+}) septet spin exohedral clusters at B3LYP/DEF level of theory. (Vertical Arrow represents highest energy SOMO)

FigureS7. Molecular orbital pictures of valence singly occupied molecular orbitals (SOMOs) of septet spin exohedral $PuB_{12}H_{12}$ at B3LYP/DEF level of theory.

Table S1. Relative Energy (RE, in eV) of Singlet, Triplet, Quintet, and Septet Spin of Endohedral clusters with respect to corresponding Septet Spin Exohedral Cluster using Different DFT methods with and without symmetry

Endohedral Systems	**RE**			
	UNP0	**UNP2**	**UNP4**	**UNP6**
C_{3v}-Symmetry				
Pu@$Al_{12}H_{12}$				
PBE	0.82	1.27	...*	1.08
B3LYP	2.57	2.87	2.64	2.27
M06-2X	4.25	3.68	2.80	1.95
TPSSH	1.14	1.60	1.50	1.13
Sm@$Al_{12}H_{12}$				
PBE	6.09	...*	...*	2.58
B3LYP	7.52	6.56	4.96	3.72
M06-2X	10.46	8.79	5.56	3.82
TPSSH	6.38	5.35	...*	2.72
C_1-Symmetry				
Pu@$Al_{12}H_{12}$				
B3LYP	2.58	2.89	2.62	2.28
M06-2X	4.29	3.71	2.87	1.98
Sm@$Al_{12}H_{12}$				
B3LYP	7.55	6.57	4.99	3.74
M06-2X	10.42	8.04	5.60	3.83

*Geometry is not converged properly

Table S2. Relative Energy (RE, in eV) of Singlet, Triplet and Quintet Spin of Exohedral clusters with respect to corresponding Septet Spin Exohedral Cluster using Different DFT methods with and without symmetry

Exohedral Systems	RE			
	UNP0	UNP2	UNP4	UNP6
C_{3v}_Symmetry				
Pu@$Al_{12}H_{12}$				
PBE	3.71	... *	...*	0.00
B3LYP	3.82	2.38	1.40	0.00
M06-2X	5.59	3.41	1.56	0.00
TPSSH	3.61	2.08	....*	0.00
Sm@$Al_{12}H_{12}$				
PBE	5.69	3.01	... *	0.00
B3LYP	5.38	4.62	2.53	0.00
M06-2X	7.62	7.69	1.86	0.00
TPSSH	5.42	3.02	...*	0.00
Pu@$B_{12}H_{12}$				
PBE	4.08	...*	...*	0.00
B3LYP	6.37	3.07	2.67	0.00
M06-2X	5.74	4.50	3.09	0.00
TPSSH	3.78	3.26	...*	0.00
Sm@$B_{12}H_{12}$				
PBE	5.77	...*	...*	0.00
B3LYP	9.88	4.56	2.53	0.00
M06-2X	7.61	5.52	3.56	0.00
TPSSH	5.42	4.59	...*	0.00
C_1-Symmetry				
Sm@$Al_{12}H_{12}$				
B3LYP	3.83	2.39	1.44	0.00
M06-2x	5.78	3.43	1.57	0.00
Sm@$Al_{12}H_{12}$				
B3LYP	5.39	3.33	2.22	0.00
M06-2x	7.57	5.44	3.52	0.00
Pu@$B_{12}H_{12}$				
B3LYP	4.08	2.36	1.17	0.00
M06-2x	5.81	3.00	1.52	0.00
Sm@$B_{12}H_{12}$				
B3LYP	5.39	4.01	2.16	0.00
M06-2x	7.55	4.23	2.93	0.00

*Geometry is not converged properly

Table S3. Calculated Values of the Optimized Bond Lengths (R, in Å) of bare $Al_{12}H_{12}^{2-}$ and Exohedral ($An@Al_{12}H_{12}^{2-}$ and $Ln@Al_{12}H_{12}^{2-}$) Clusters in Septet Spin State using B3LYP/DEF Method

Clusters	At Metal Doped Triangular Face			$^{a}R_{(cage-dia)}$
	$R_{(Al-Al)}$	$R_{(M-H)}$	$R_{(Al-H)}$	
$Al_{12}H_{12}^{2-}$	2.704	...	1.605	5.144
$Np@Al_{12}H_{12}^{-}$	2.699	2.483	1.642	5.062 (5.216)
$Pu@Al_{12}H_{12}$	2.732	2.320	1.667	5.040 (5.262)
$Am@Al_{12}H_{12}^{+}$	2.691	2.353	1.655	5.099 (5.271)
$Pm@Al_{12}H_{12}^{-}$	2.700	2.560	1.637	5.052 (5.220)
$Sm@Al_{12}H_{12}$	2.730	2.361	1.663	5.040 (5.258)
$Eu@Al_{12}H_{12}^{+}$	2.688	2.380	1.651	5.099 (5.266)

Table S4. Calculated Values of the Optimized bond lengths (R, in Å) of bare $B_{12}H_{12}^{2-}$ Cluster and Exohedral ($An@B_{12}H_{12}^{2-}$ and $Ln@B_{12}H_{12}^{2-}$) Clusters in Septet Spin State using B3LYP/DEF Method

Clusters	At Metal Doped Triangular Face			$^{a}R_{(cage-dia)}$
	$R_{(B-B)}$	$R_{(M-H)}$	$R_{(B-H)}$	
$B_{12}H_{12}^{2-}$	1.783	...	1.201	3.392
$Np@B_{12}H_{12}^{-}$	1.784	2.422	1.218	3.365 (3.408)
$Pu@B_{12}H_{12}$	1.808	2.290	1.232	3.364 (3.420)
$Am@B_{12}H_{12}^{+}$	1.789	2.348	1.221	3.426 (3.454)
$Pm@B_{12}H_{12}^{-}$	1.783	2.437	1.216	3.365 (3.407)
$Sm@B_{12}H_{12}$	1.803	2.305	1.229	3.364 (3.417)
$Eu@B_{12}H_{12}^{+}$	1.787	2.352	1.218	3.419 (3.454)

Table S5. Comparison of Calculated Values of Optimized Bond Length ($R_{(M-Al)}$, in Å), Binding Energy (BE, in eV), HOMO−LUMO Energy Gap (ΔE_{Gap}, in eV), NPA Charge on Doped ion (q_M, in e) and Total Spin Population (N_S) of Exohedral Pu@$Al_{12}H_{12}$ and Sm@$Al_{12}H_{12}$ Clusters with and without Symmetry in Septet Spin State using Different DFT Methods. Atomic f-Population (nf) of An/Ln is Provided in Parenthesis.

Cluster	Sym	$R_{(M-Al)}$	BE	ΔE_{Gap}	q_M	N_S (nf)
$Al_{12}H_{12}^{2-}$						
PBE	I_h	...	...	2.511	...	...
B3LYP	I_h	...	...	3.698	...	...
M06-2X	I_h	...	...	4.968	...	...
TPSSH	I_h	...	...	2.969	...	...
Pu@$Al_{12}H_{12}$						
PBE	C_{3v}	3.007	-17.57	0.128	1.048	6.163 (5.805)
B3LYP	C_{3v}	3.070	-16.79	2.210	1.202	6.170 (5.869)
M06-2X	C_{3v}	3.077	-16.91	3.723	1.329	6.137 (5.919)
TPSSH	C_{3v}	2.995	-17.17	1.420	1.138	6.212 (5.869)
Sm@$Al_{12}H_{12}$						
PBE	C_{3v}	3.063	-16.71	0.353	1.260	6.151 (5.950)
B3LYP	C_{3v}	3.106	-16.34	2.497	1.367	6.138 (5.986)
M06-2X	C_{3v}	3.118	-16.46	3.888	1.472	6.118 (5.984)
TPSSH	C_{3v}	3.069	-16.59	2.184	1.346	6.150 (5.963)
$Al_{12}H_{12}^{2-}$						
Without Symmetry Constrain						
B3LYP	C_1	...	...	3.696	...	...
M06-2X	C_1	...	...	4.965	...	...
Pu@$Al_{12}H_{12}$						
B3LYP	C_1	3.052	-16.80	2.211	1.190	6.190 (5.879)
M06-2X	C_1	3.068	-16.95	3.811	1.333	6.152 (5.960)
Sm@$Al_{12}H_{12}$						
B3LYP	C_1	3.100	-16.37	2.508	1.363	6.142 (5.983)
M06-2X	C_1	3.113	-16.46	3.904	1.468	6.122 (5.990)

Table S6. Comparison of Calculated Values of Optimized Bond Length ($R_{(M-B)}$, in Å), Binding Energy (BE, in eV), HOMO−LUMO Energy Gap (ΔE_{Gap}, in eV), NPA Charge on Doped ion (q_M, in e) and Total Spin Population (N_S) of Exohedral $Pu@B_{12}H_{12}$ and $Sm@B_{12}H_{12}$ Clusters with and without Symmetry in Septet Spin State using Different DFT Methods. Atomic f-Population (nf) of An/Ln is Provided in Parenthesis.

Clusters	Sym	$R_{(M-B)}$	BE	ΔE_{Gap}	q_M	N_S (nf)
$B_{12}H_{12}^{2-}$						
PBE	I_h	...	...	5.437	...	...
B3LYP	I_h	...	...	6.571	...	...
M06-2X	I_h	...	...	8.240	...	...
TPSSH	I_h	...	...	6.157	...	...
$Pu@B_{12}H_{12}$						
PBE	C_{3v}	2.584	-18.54	0.147	1.493	6.131 (5.782)
B3LYP	C_{3v}	2.636	-17.81	2.081	1.602	6.112 (5.859)
M06-2X	C_{3v}	2.639	-18.01	4.841	1.685	6.088 (5.927)
TPSSH	C_{3v}	2.598	-18.23	1.315	1.580	6.131 (5.851)
$Sm@B_{12}H_{12}$						
PBE	C_{3v}	2.610	-17.85	0.362	1.575	6.114 (5.950)
B3LYP	C_{3v}	2.646	-17.49	3.282	1.647	6.097 (5.970)
M06-2X	C_{3v}	2.657	-17.55	5.136	1.719	6.083 (5.979)
TPSSH	C_{3v}	2.613	-17.82	2.312	1.631	6.111 (5.957)
Without Symmetry Constrain						
$B_{12}H_{12}^{2-}$						
B3LYP	C_1	...	...	6.576	...	...
M06-2X	C_1	...	...	8.243	...	...
$Pu@B_{12}H_{12}$						
B3LYP	C_1	2.637	-17.80	2.027	1.606	6.108 (5.880)
M06-2X	C_1	2.638	-18.01	4.863	1.686	6.085 (5.927)
$Sm@B_{12}H_{12}$						
B3LYP	C_1	2.650	-17.47	3.295	1.648	6.094 (5.966)
M06-2X	C_1	2.654	-17.54	5.153	1.719	6.081 (5.980)

Table S7. Comparison of Calculated Values of the Optimized Bond Lengths ($R_{(M-Al)}$, in Å), Binding Energy (BE, in eV), HOMO-LUMO Energy Gap (ΔE_{Gap}, eV) and Total Spin Population (N_S) of Endohedral $Pu@Al_{12}H_{12}$ and $Sm@Al_{12}H_{12}$ Clusters with and without Symmetry in Septet Spin State using Different DFT Methods. Atomic f-Population (nf) of An/Ln is Provided in Parenthesis.

Cluster	Sym	$R_{(M-Al)}$	BE	ΔE_{Gap}	N_S (nf)
$Al_{12}H_{12}^{2-}$					
PBE	I_h	...	...	2.511	...
B3LYP	I_h	...	...	3.698	...
M06-2X	I_h	...	...	4.968	...
TPSSH	I_h	...	...	2.969	...
$Pu@Al_{12}H_{12}$					
PBE	C_{3v}	2.774	-16.49	0.077	5.717 (5.391)
B3LYP	C_{3v}	2.782	−14.52	2.045	5.718 (5.466)
M06-2X	C_{3v}	2.754	-14.97	4.013	5.861 (5.601)
TPSSH	C_{3v}	2.762	-16.04	1.417	5.743 (5.453)
$Sm@Al_{12}H_{12}$					
PBE	C_{3v}	2.772	-14.13	0.345	6.015 (5.745)
B3LYP	C_{3v}	2.781	−12.62	2.907	6.033 (5.794)
M06-2X	C_{3v}	2.759	-12.64	4.793	6.149 (5.902)
TPSSH	C_{3v}	2.760	-13.88	2.268	6.055 (5.770)
Without Symmetry Constrain					
$Al_{12}H_{12}^{2-}$					
B3LYP	C_1	...	...	3.696	...
M06-2X	C_1	...	...	4.965	...
$Pu@Al_{12}H_{12}$					
B3LYP	C_1	2.781	-14.51	2.051	5.717 (5.466)
M06-2X	C_1	2.749	-14.97	4.007	5.859 (5.600)
$Sm@Al_{12}H_{12}$					
B3LYP	C_1	2.781	−12.63	2.905	6.032 (5.793)
M06-2X	C_1	2.758	-12.63	4.789	6.149 (5.902)

Table S8. Comparison of Binding Energy (BE, in eV), HOMO−LUMO Energy Gap (ΔE_{Gap}, in eV) and $<S^2>$ value of Exohedral $An@Al_{12}H_{12}^{2-}$ and $Ln@Al_{12}H_{12}^{2-}$ Clusters in Septet Spin State using B3LYP/DEF, PBE/DEF, M06-2X/DEF and TPSSH/DEF Methods

Cluster	PBE	B3LYP	M06-2X	TPSSH
$Np@Al_{12}H_{12}^{-}$				
$<S^2>$	12.024	12.011	12.008	12.021
BE	-7.88	-7.26	-7.70	-7.83
ΔE_{Gap}	0.028	1.530	0.503	0.730
$Pu@Al_{12}H_{12}$				
$<S^2>$	12.027	12.017	12.015	12.032
BE	-17.40	-16.79	-16.91	-17.17
ΔE_{Gap}	0.128	2.210	3.723	1.420
$Am@Al_{12}H_{12}^{+}$				
$<S^2>$	12.792	13.027	13.026	13.033
BE	-34.50	-33.58	-33.66	-33.82
ΔE_{Gap}	0.095	1.146	2.487	0.563
$Pm@Al_{12}H_{12}^{-}$				
$<S^2>$	12.010	12.006	12.009	12.009
BE	-7.52	-7.04	-7.73	-7.50
ΔE_{Gap}	0.301	1.442	0.623	0.808
$Sm@Al_{12}H_{12}$				
$<S^2>$	12.015	12.011	12.014	12.014
BE	-16.71	-16.34	-16.46	-16.59
ΔE_{Gap}	0.353	2.497	3.888	2.184
$Eu@Al_{12}H_{12}^{+}$				
$<S^2>$	13.017	13.023	13.029	13.028
BE	-36.27	-35.43	-35.67	-35.75
ΔE_{Gap}	0.096	1.185	2.495	0.784

Table S9. Comparison of Binding Energy (BE, in eV), HOMO−LUMO Energy Gap (ΔE_{Gap}, in eV) and $<S^2>$ value of Exohedral $An@B_{12}H_{12}^{2-}$ and $Ln@B_{12}H_{12}^{2-}$ Clusters in Septet Spin State using B3LYP/DEF, PBE/DEF, M06-2X/DEF and TPSSH/DEF Methods

Cluster	PBE	B3LYP	M06-2X	TPSSH
$Np@B_{12}H_{12}^{-}$				
$<S^2>$	12.008	12.005	12.005	12.008
BE	-8.98	-8.55	-8.88	-9.01
ΔE_{Gap}	0.065	1.238	0.301	0.680
$Pu@B_{12}H_{12}$				
$<S^2>$	12.016	12.011	12.010	12.014
BE	-18.38	-17.81	-18.01	-18.23
ΔE_{Gap}	0.147	2.081	4.841	1.315
$Am@B_{12}H_{12}^{+}$				
$<S^2>$	12.720	13.009	13.011	12.964
BE	-34.24	-33.12	-33.18	-33.59
ΔE_{Gap}	0.138	1.671	4.066	0.658
$Pm@B_{12}H_{12}^{-}$				
$<S^2>$	12.006	12.004	12.008	12.005
BE	-8.83	-8.43	-9.02	-8.87
ΔE_{Gap}	0.380	1.557	1.006	1.044
$Sm@B_{12}H_{12}$				
$<S^2>$	12.011	12.008	12.011	12.010
BE	-17.87	-17.49	-17.55	-17.82
ΔE_{Gap}	0.402	3.282	5.136	2.312
$Eu@B_{12}H_{12}^{+}$				
$<S^2>$	12.955	12.955	13.017	13.012
BE	-36.11	-35.11	-35.31	-35.68
ΔE_{Gap}	0.177	2.085	4.053	1.378

Table S10. Analysis of the Orbitals Compositions of Septet Spin Endohedral Pu@$Al_{12}H_{12}$ Cluster in C_{3v} Symmetry Using PBE/TZ2P Method

Energy (eV)	[a]Occu	[b]IRR_SR	[c]IRR_RECP	MO(%) metal/cage
-12.913	2.00	10A1.g	22a1	66.58% Pu(s) +33% Cage
-10.979	2.00	11E1.u:1	25e-2	7.5% Pu(p) + 92% cage
-10.979	2.00	11E1.u:2	25e-1	7.5% Pu(p) + 92% cage
-10.979	2.00	9A2.u	23a1	8.5% Pu(p) + 91.5% cage
-10.116	2.00	11E1.g:1	26e-2	12.52% Pu(dyz)+ 87.48% cage
-10.116	2.00	11E1.g:2	26e-1	12.52% Pu(dxz)+ 87.48% cage
-10.086	2.00	12E1.g:1	27e-2	45.53% Pu(dx2-y2)+54.47% cage
-10.086	2.00	12E1.g:2	27e-2	45.53% Pu(dxy)+54.47% cage
-10.069	2.00	11A1.g	24a1	45.75% Pu(dz2)+54.26% cage
-9.157	2.00	12E1.u:1	28e-2	cage
-9.157	2.00	12E1.u:2	28e-1	cage
-9.137	2.00	10A2.u	25a1	cage
-8.491	2.00	12A1.g	26a1	21.96% Pu(s) +78.04% Cage
-7.624	2.00	13E1.g:1	29e-2	18.49% Pu (dyz)+81.51% Cage
-7.624	2.00	13E1.g:2	29e-1	18.49% Pu (dxz)+81.51% Cage
-7.607	2.00	13A1.g	27a1	19.98% Pu (dz2) + 80.02% cage
-7.597	2.00	14E1.g:1	30e-2	18.27% Pu(dx2-y2)+ 81.73%cage
-7.597	2.00	14E1.g:2	30e-1	18.27% Pu(dxy)+ 81.73%cage
-7.309	2.00	11A2.u	28a1	14.05% Pu(pz)+ 85.95%cage
-7.301	2.00	13E1.u:1	31e-2	13.54% Pu(px) + 86.46%cage
-7.301	2.00	13E1.u:2	31e-1	13.54% Pu(py) + 86.46%cage
-6.207	2.00	14E1.u:1	32e-2	24.61% Pu(f) + 75.39%cage
-6.207	2.00	14E1.u:2	32e-1	24.61% Pu(f) + 75.39%cage
-6.172	2.00	3A1.u	5a2	24.32%Pu(f) + 75.68%cage
-6.140	2.00	12A2.u	29a1	24.31%Pu(f) + 75.67%cage
-5.251	1.00	15E1.u:1	33e-2	75.08%Pu(f) + 24.92%cage
-5.251	1.00	15E1.u:2	33e-1	75.08%Pu(f) + 24.92%cage
-5.003	1.00	13A2.u	30a1	70.88%Pu(f) + 29.12%cage
-4.021	1.00	16E1.u:1	34e-2	71.98%Pu(f) + 28.02%cage
-4.021	1.00	16E1.u:2	34e-1	71.98%Pu(f) + 28.02%cage
-3.947	1.00	4A1.u	6a2	74.09%Pu(f) + 25.91%cage-HOMO
-3.895	0.00	14A2.u	31a1	73.27%Pu(f) + 26.73%cage-LUMO

[a]Occu = Occupation of orbital
[b]IRR_SR= Irreducible representation of molecular orbital using scalar relativistic ZORA approach
[c]IRR_ECP= Irreducible representation of molecular orbital using relativistic ECP

Table S11. Analysis of the Orbitals Compositions of Septet Spin Endohedral $Sm@Al_{12}H_{12}$ Cluster in C_{3v} Symmetry Using PBE/TZ2P Method

Energy (eV)	[a]Occ	[b]IRR_SR	[c]IRR_RECP	Contribution
-12.783	2.00	8A1.g	22a1	56.64 % Pu(s) + 43.36% cage
-11.088	2.00	8A2.u	23a1	20.71% Pu(pz) + 79.29% cage
-11.086	2.00	10E1.u:1	25e-2	19.43% Pu(px) + 80.57 % cage
-11.086	2.00	10E1.u:2	25e-1	19.43% Pu(py) + 80.57 % cage
-10.062	2.00	9E1.g:1	26e-2	10.56/5.42 % Sm (dyz) + 89.44/94.58 % cage
-10.062	2.00	9E1.g:2	26e-1	10.56/5.42 % Sm (dzx) + 89.44/94.58 % cage
-10.044	2.00	10E1.g:1	27e-2	10.56/5.42 % Sm (dx2-y2) + 89.44/94.58 %cage
-10.044	2.00	10E1.g:2	27e-2	10.56/5.42 % Sm (dxy) + 89.44/94.58 % cage
-10.042	2.00	9A1.g	24a1	11.04/5.08% Sm(dz2) + 88.96/ 94.92 % cage
-9.144	2.00	11E1.u:1	28e-2	cage
-9.144	2.00	11E1.u:2	28e-1	cage
-9.130	2.00	9A2.u	25a1	cage
-8.385	2.00	10A1.g	26a1	14.93% Sm(s) + 85.07% cage
-7.533	2.00	11E1.g:1	29e-2	13.3 % Sm(dyz) + 86.7 % cage
-7.533	2.00	11E1.g:2	29e-1	13.3 % Sm(dxz) + 86.7 % cage
-7.524	2.00	11A1.g	27a1	13.7 % Sm(dz2) + 80.46 % cage
-7.517	2.00	12E1.g:1	30e-2	13.3 % Sm(dx2-y2) + 86.7 % cage
-7.517	2.00	12E1.g:2	30e-1	13.3 % Sm(dxy) + 86.7 % cage
-7.432	2.00	10A2.u	28a1	19.54% Sm(pz) + 80.46 % cage
-7.424	2.00	12E1.u:1	31e-2	18.99% Sm(px) + 81.01 % cage
-7.424	2.00	12E1.u:2	31e-1	18.99% Sm(py) + 81.01 % cage
-5.985	2.00	13E1.u:1	32e-2	15.48% Sm(f) + 84.52 % cage
-5.985	2.00	13E1.u:2	32e-1	15.48% Sm(f) + 84.52 % cage
-5.976	2.00	3A1.u	5a2	14.48% Sm(f) + 85.52 % cage
-5.948	2.00	11A2.u	29a1	12.79% Sm(f) + 87.21 % cage
-5.096	1.00	14E1.u:1	33e-2	16.16% Sm(f) + 83.84 % cage
-5.096	1.00	14E1.u:2	33e-1	16.16% Sm(f) + 83.84 % cage
-4.650	1.00	12A2.u	30a1	79.83% Sm(f) + 20.17 % cage
-4.342	1.00	4A1.u	6a2	84.09% Sm(f) + 15.91 % cage
-4.335	1.00	15E1.u:1	34e-2	83.66% Sm(f) + 16.34 % cage
-4.335	1.00	15E1.u:2	34e-1	83.66% Sm(f) + 16.34 % cage-HOMO
-4.186	0.00	13A2.u	31a1	85.3% Sm(f) + 14.70 % cage-LUMO

[a]Occu = Occupation of orbital
[b]IRR_SR= Irreducible representation of molecular orbital using scalar relativistic ZORA approach
[c]IRR_ECP= Irreducible representation of molecular orbital using relativistic ECP

Geometry	Inital_Geom	Final_Geom
STR1	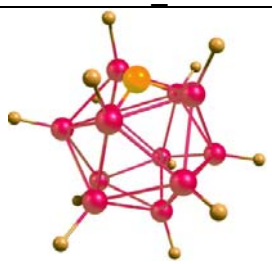	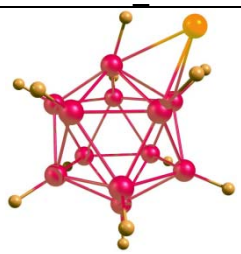
STR2	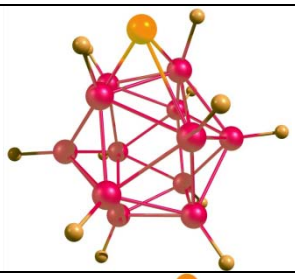	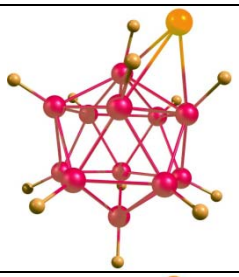
STR3	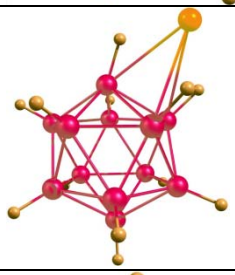	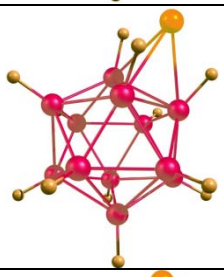
STR6	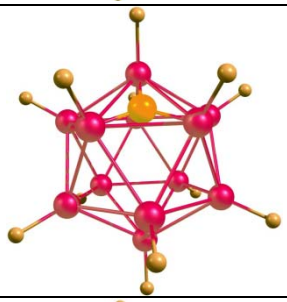	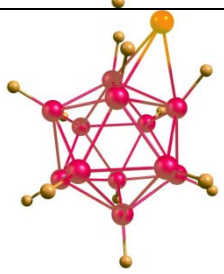
STR4	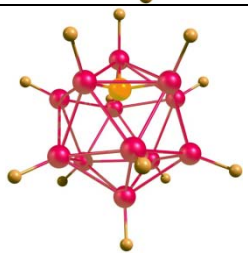	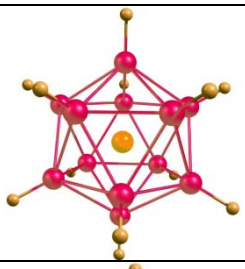
STR5		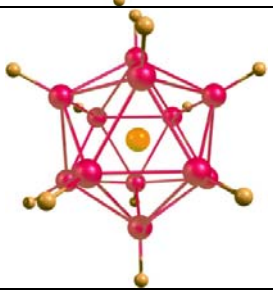

Figure S1. Optimized exohedral and endohedral cluster using different initial geometry without any symmetry constrain at B3LYP/DEF level of theory.

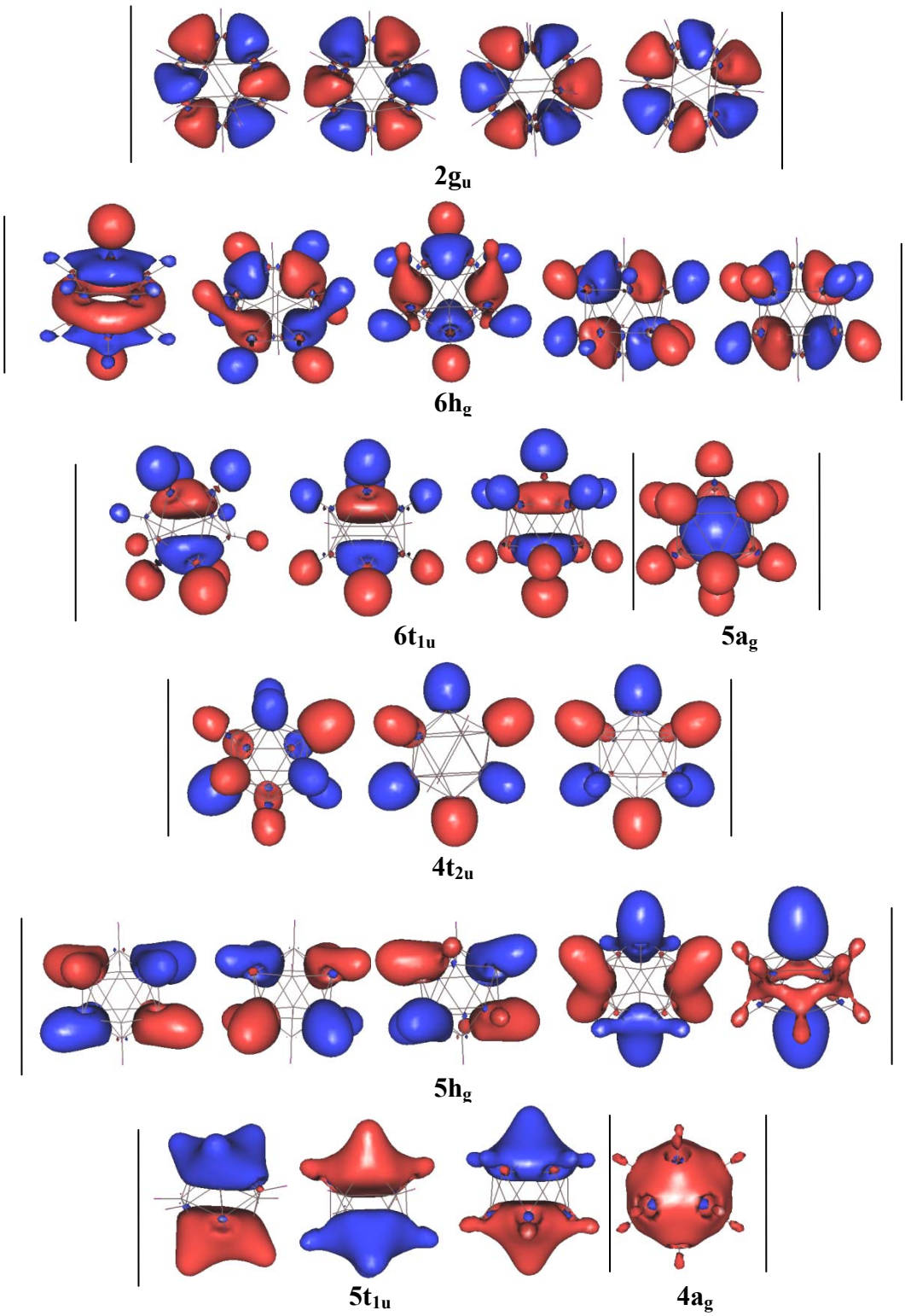

Figure S2. Molecular orbital pictures of $Al_{12}H_{12}^{2-}$ cluster in I_h symmetry using B3LYP/DEF Method

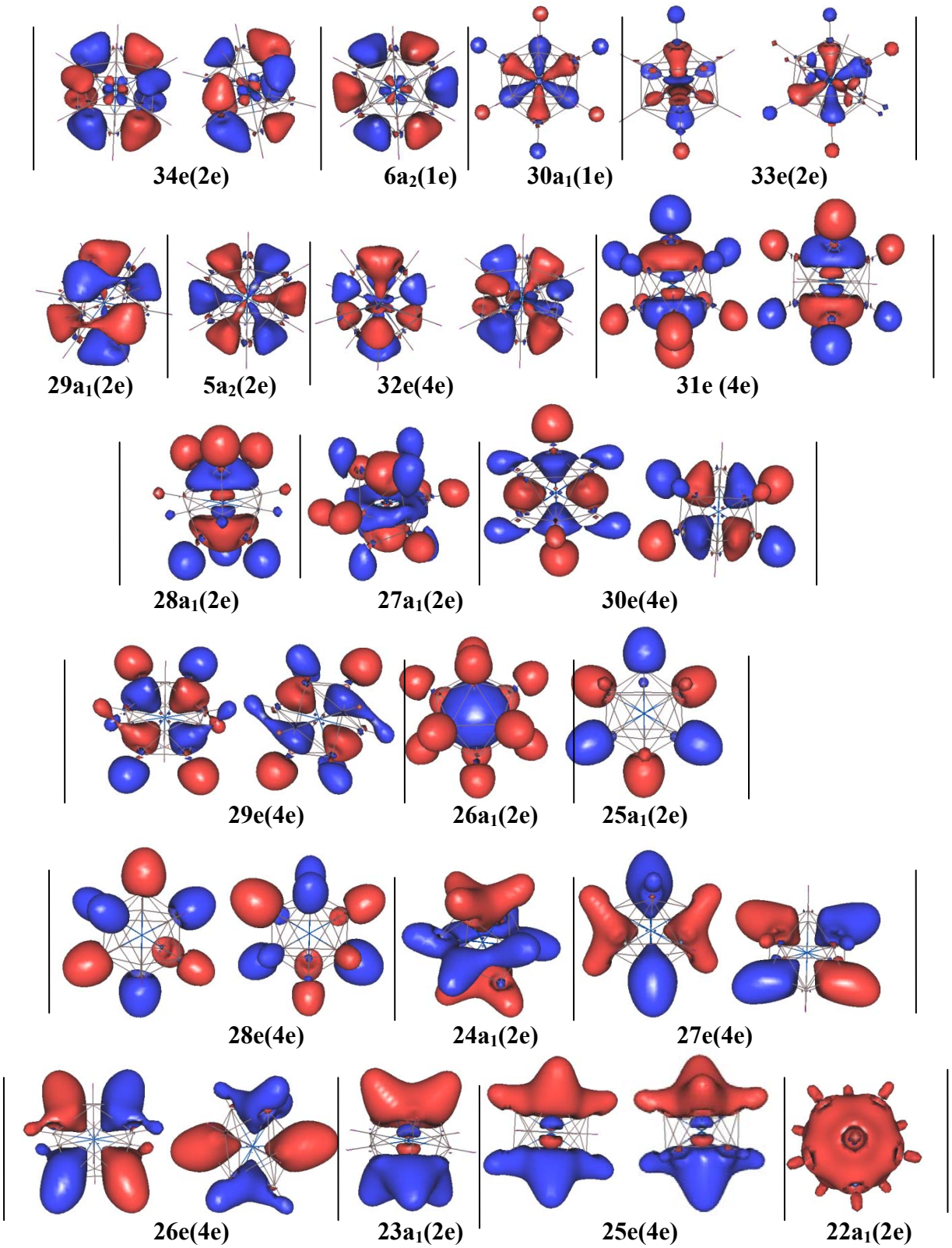

Figure S3. Molecular orbital pictures of endohedral $Pu@Al_{12}H_{12}$ cluster in C_{3v} symmetry using B3LYP/DEF Method. (Blue text represents MOs with metal-cage overlap, red text represent pure cage MOs, green text represent MOs with negligible mixing of cage with the metal)

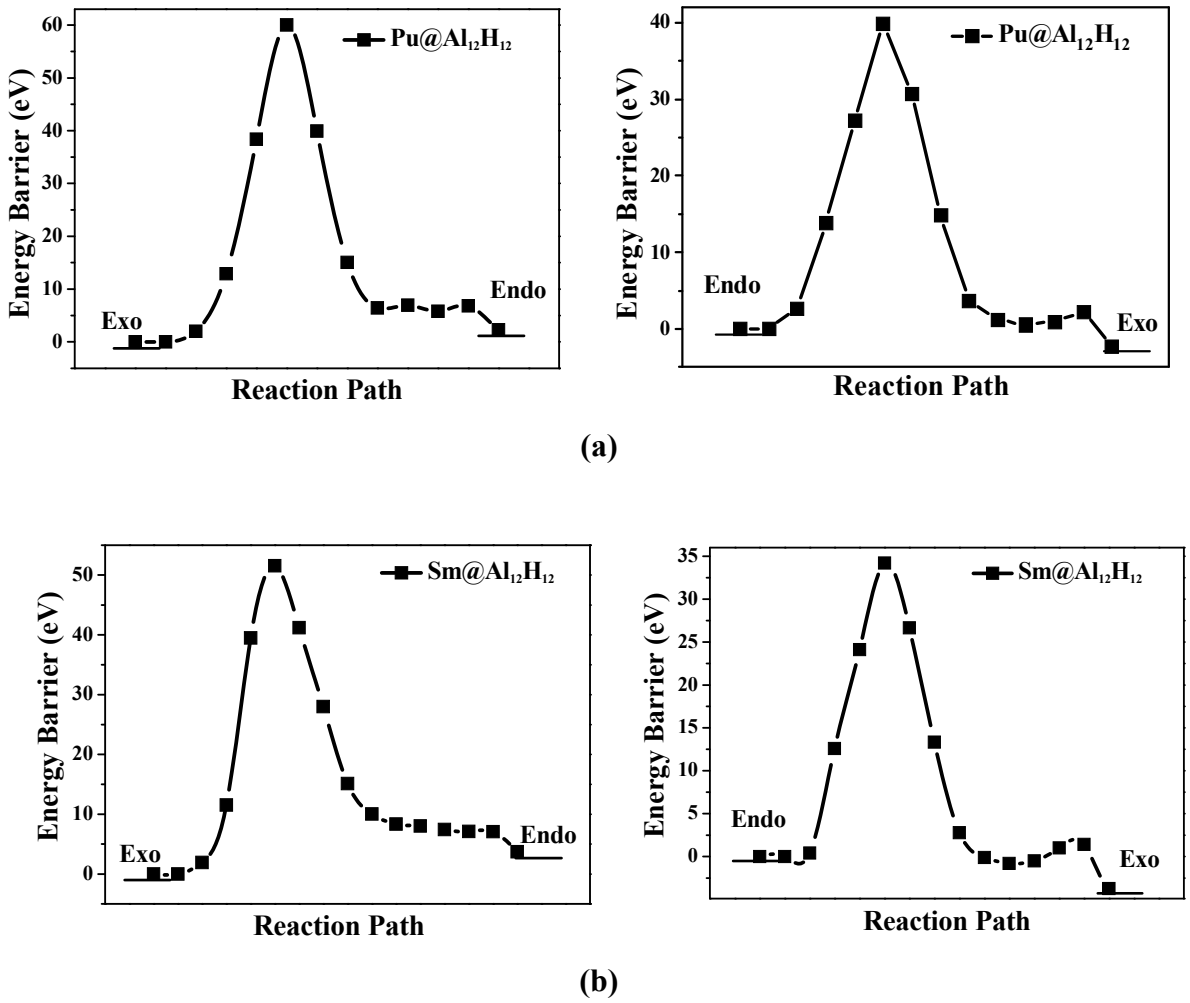

Figure S4. Energy barrier plots of exohedral and endohedral a) $Pu@Al_{12}H_{12}$ and b) $Sm@Al_{12}H_{12}$ clusters, respectively, obtained using B3LYP/DEF method.

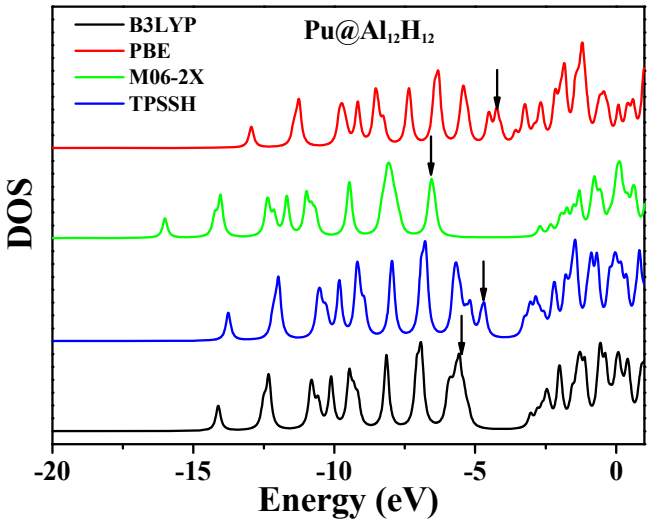

(a)

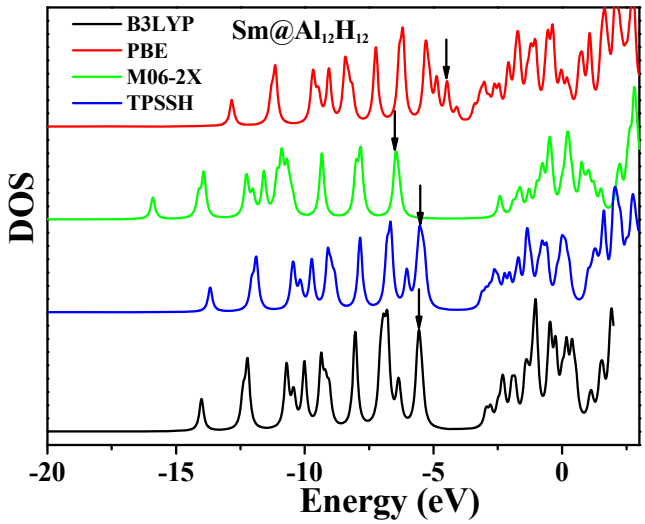

(b)

Figure S5. Density of state (DOS) plots of (a) Pu@$Al_{12}H_{12}$ and (b) Sm@$Al_{12}H_{12}$, septet spin exohedral clusters at B3LYP/DEF, PBE/DEF, M06-2X/DEF and TPSSH/DEF level of theory.

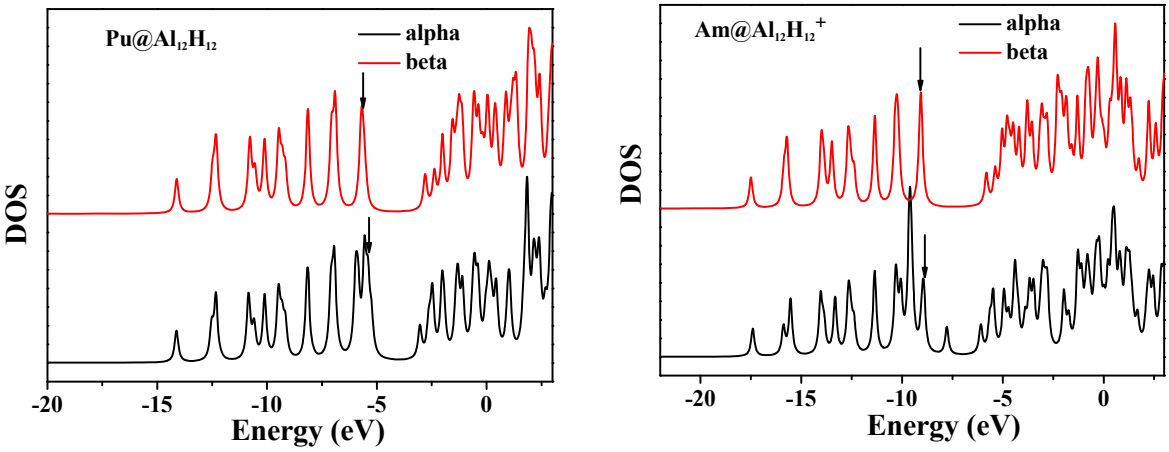

(a)

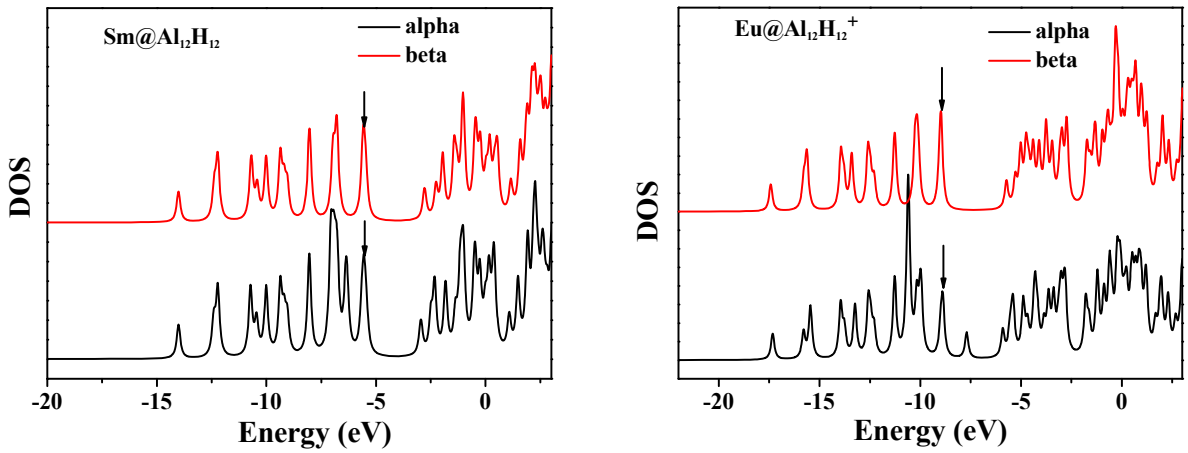

(b)

Figure S6. Density of state (DOS) of spin up (alpha) and spin down (beta) plots of (a) $An@Al_{12}H_{12}^{2-}$ ($An = Pu^{2+}$, Am^{3+}) and (b) $Ln@Al_{12}H_{12}^{2-}$ ($Ln = Sm^{2+}$, Eu^{3+}) septet spin exohedral clusters at B3LYP/DEF level of theory. (Vertical Arrow represents highest energy SOMO)

MOs of $PuB_{12}H_{12}$	SR	SOC
SOMO	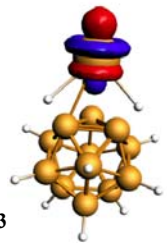 f:z^3	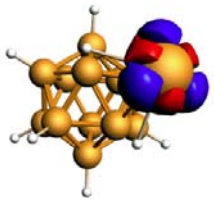
SOMO-1	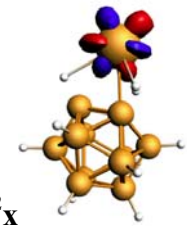 f:z^2x	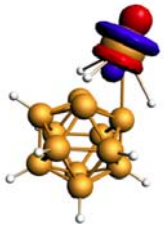
SOMO-2	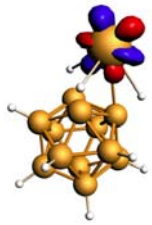 f:z^2y	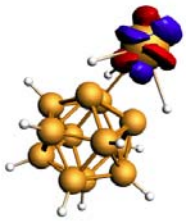
SOMO-3	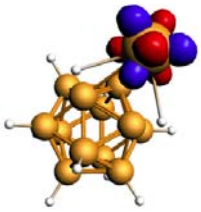 f:z	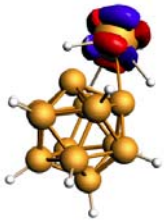
SOMO-4	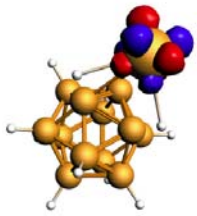 f:xyz	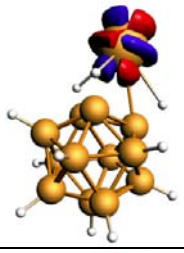
SOMO-5	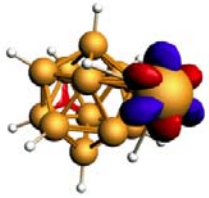 f:x	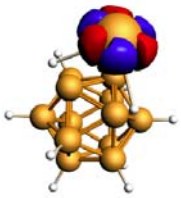

FigureS7. Molecular orbital pictures of valence singly occupied molecular orbitals (SOMOs) of septet spin exohedral $PuB_{12}H_{12}$ at B3LYP/DEF level of theory